International Scholars Journals

African Journal of Medicine and Surgery ISSN 2756-3324 Vol. 11 (8), pp. 001-012, August, 2024. Available online at www.internationalscholarsjournals.org © International Scholars Journals

Full Length Research Paper

Osteoinductive Properties of 17% Chitosan-Enhanced Bioactive Glass in Bone Regeneration: Insights from a Rat Model Study

Samira Jebahi[1,2]*, Hassane Oudadesse[1], Bui XV[1], Hassib Keskes[3], Tarek Rebai[4], Abdelfattah el Feki[2] and Hafed el Feki[5]

[1]Université de Rennes 1, UMR CNRS 6226, Campus de Beaulieu, 263 av. du Général Leclerc, 35042 Rennes, France.
[2]Animal Ecophysiology Laboratory, Sciences Faculty of Sfax, Department of Life Sciences Sfax, Tunisia.
[3]Laboratory of Orthopaedic and Traumatology, Medicine Faculty of Sfax, Sfax, Tunisia.
[4]Laboratory of Histology, Medicine Faculty, Sfax, Tunisia.
[5]Laboratory of Science Materials and Environment Faculty, Sfax, Tunisia.

Accepted 11 April, 2024

Bone loss due to skeletal trauma or metabolic diseases often necessitates bone grafting. This study evaluates the effectiveness of a bioactive glass-chitosan composite (BG-CH) created through a freeze-drying method. The composite, containing 17% wt% chitosan, was implanted in the femoral condyle of ovariectomized rats. The resected bone samples underwent analysis using various physicochemical techniques, including Fourier transform infrared spectroscopy (FT-IR), X-ray diffraction (XRD), scanning electron microscopy (SEM), and energy-dispersive X-ray spectroscopy (EDX). After two weeks, the spectrum of the implanted sample showed two significant absorption bands at 932 and 1036 cm-1, linked to (Si-O-Si) groups, which disappeared by 15 days post-surgery. These bands were replaced at 30 days by peaks at 601 and 564 cm-1, indicating the presence of phosphate groups from bone apatite. After four weeks, peaks at 31.6° and 25.8° (2θ) were observed, reflecting the degradation of BG-CH, which coincided with the replacement of the implant by bone cells. Our findings suggest that the addition of 17% wt% chitosan to the bioactive glass matrix significantly enhances bioactivity and osteoinductive properties, positioning BG-CH as a promising biomaterial for biomedical applications.

Key words: Chitosan-glasses, biomineralization, osteoinductivity, biomedical applications, bone defect healing.

INTRODUCTION

One of the present trends in implantable applications requires materials derived from nature. Natural materials have been shown to promote healing at a faster rate and are expected to exhibit greater compatibility with bone (Zhang et al., 2010). Recently, chitosan has played a major role in bone tissue engineering, being a natural polymer obtained from chitin (Chang et al., 2008), which is found in the major component of crustacean exoskeleton. It has attractive properties such as biocompatibility, wound healing and antibacterial activities as well as drug delivery systems (Rani et al., 2010; Viral et al., 2012). I*n vitro* behavior of hydrxyapatite-chitosan (HAP-CH) was performed in a simulated body fluid (SBF) to induce the formation of bone-like apatite layer onto their surfaces (Liuy et al., 2009). While chitosan has been extensively investigated for bone repair, there has been relatively little research on the application in the repair of osteoporosis tissues. In the medical field, among the most common drugs developed for treatment of osteoporosis in clinical practice, we noted estrogens, bisphosphonates and calcitonin. In postmenopausal women, estrogen as hormone replacement is often prescribed for the

*Corresponding author. E-mail: jbahisamira@yahoo.fr. Tel: +21697622227

prevention of osteoporosis (Lee et al., 1999; Ha et al., 2001), but it can result in an increased risk of endometrial cancer (Grady et al., 199l). Other adverse effects involve gastrointestinal disturbances and risk for osteonecrosis in the mandible and maxilla with bisphosphonates. Recent studies in ovariectomized rats showed that oral administration of chitosan prevents bone demineralization (Iwata et al., 2005). When applied to bone defects, chitosan was found to improve osteogenesis and angiogenic activity (Muzzarelli et al., 2002). However, the poorer mechanical strength of CH presents one of the main limitations (Malafaya et al., 2008). Accordingly, inorganic–organic composites for bone repair should be developed and are expected to enhance the mechanical properties of the polymer matrix with particle reinforcement. Within a current strategy, the mechanical properties of porous chitosan/hydroxyapatite nano-composites proved to be satisfactory when implanted in the rat (Kashiwazaki et al., 2009). Differentiation and activity of human preosteoclasts were enhanced when tested on chitosan enriched calcium phosphate cement (Rochet et al., 2009). Moreover, several studies have confirmed chitosan usefulness when interacted with gelatin/nano-bioactive glass (Petera et al., 2010). Bearing all these considerations in mind, the purpose of this study was to evaluate the performance of BG-CH produced by freeze-drying technique in the quaternary system (SiO_2-CaO-Na_2O-P_2O_5). An experimental study on an ovariectomised rat model would be useful to assess the efficacy of BG-CH in the repair of bone defect compared with BG. This system should try to meet the key of an ideal design: A porous structure with adequate morpho-logical characteristics, and an *in vivo* biocompatibility.

MATERIALS AND METHODS

Biomaterials synthesis

BG-CH was elaborated by freeze-drying method. First, the BG particles were synthetised as described in Dietrich et al. (2009) via the melting method. Then they were suspended in the prepared chitosan solution and stirred for 2 h by using magnetic agitation at 1200 (rpm). The biocomposite contained 17 wt% of CH polymer. The mixture of BG and CH polymer was solidified by liquid azotes and transferred immediately for freeze-drying at -60°C for 24 h to remove the solvents. To neutralize the radicals of acetic acid, the obtained biocomposite was immersed in NaOH solution, and then washed with deionised water. Eventually, the biocomposite of BG and CH polymer was frozen and freeze-dried again for 24 h to totally remove the solvent. The prepared implants were sterilized by γ-irradiation from a ^{60}Co Source gamma irradiation at a dose of 25 Gy (Equinox, UK) using standard procedures for medical devices.

Animal model

Female Wistar rats, with body weights 300 to 385 g and bred in the central animal house and obtained from the central pharmacy, Tunisia, were used in this study. The animals were fed on a pellet diet (Sicco, Sfax, Tunisia) and water *ad libitum*. All the animals were kept in climate-controlled conditions (25°C; 55% humidity; 12 h of light alternating with 12 h of darkness). The handling of the animals was approved by the Tunisian ethical committee for the care and use of laboratory animals. All rats were randomly divided into four groups (5 animals per group):

Group (I): Used as negative control (T); without ovariectomy. The femoral condyls were intact and without a surgical creation of bone defects.
Group (II): Used as positive control (OVX); with ovariectomy. Sixty days after bilateral ovariectomy, the rats developed the bone disorder and thus could be used as the animal model for osteoporosis. The femoral condyls were intact and without a surgical creation of bone defects.
Group (III); Sixty days after bilateral ovariectomy the bone defects were implanted with BG-CH (OVX -BG-CH).
Group (lV); Sixty days after bilateral ovariectomy, the bone defects were implanted with BG (OVX -BG).

Surgical and postoperative protocol

All surgical interventions were performed under general anaesthesia in aseptic conditions. Anaesthesia was induced with xylazine (7 to 10 mg/kg (i.P.) ROMPUN® 2%) and ketamine (70 to 100 mg /kg(i.m) imalgéne ®) depending on body weight. The animals underwent bilateral ovariectomy; the rats were placed for surgery in lateral recumbency and then rotated to the contralateral side during the surgical protocol. The preoperative preparation of the surgical sites was routinely performed by cleaning with 96% alcohol and antiseptic solutions (PROLABO; AnalaR Normapur®, France). The resulting bone defects were irrigated profusely with physiological saline solution (0.9 wt.% NaCl; Ref.091214; Siphal, Tunisia) to eliminate bone debris. A drilled hole, 3-mm diameter and 4-mm deep, was created on the lateral aspect of the femoral condyle using a refrigerated drill to avoid necrosis. The drill-hole was filled with 10 mg BG/BG-CH before being filled with implants; the filling was done carefully in a retrograde fashion to ensure both minimal inclusion of air bubbles and direct implant – bone contact. The closure of the wounds was performed in layers (that is, fascias and the subcutaneous tissue), using a resorbable material (Vicryl 3/0; Ethicon, Germany) in a continuous fashion. After surgery, all rats received subcutaneous analgesia (Carprofen 10 mg/kg I CRimadyl®) for three postoperative days and they were allowed unrestricted mobility; during this period, they were checked daily for clinical lameness or other complications. On days 4, 7, 15, 30 and 60 days after implant insertion, all rats were sacrificed and specimens were harvested for the following evaluation.

Biochemical assays

Biochemical analyses were carried out 60 days after the implant insertion. Blood samples were taken by cardiac puncture under light diethyl-ether anesthesia. Calcium (Ca), phosphorus (P), silicon (Si) and total alkaline phosphatase (ALP) were examined using commercial Biomaghreb kits (Tunisia).

Physicochemical analysis

The newly formed bone was analysed by SEM, using a JEOL JSM 6301F. Semi-quantitative chemical analysis was performed by EDS on implanted bone surfaces covered with a thin film gold-palladium (to avoid charge accumulation at the surface of the analysed biomaterial). Moreover, an X-ray diffraction (XRD) technique (Philips PW 3710 diffractometer) allowed the verification of the progressive similarity between the diffraction patterns of the normal

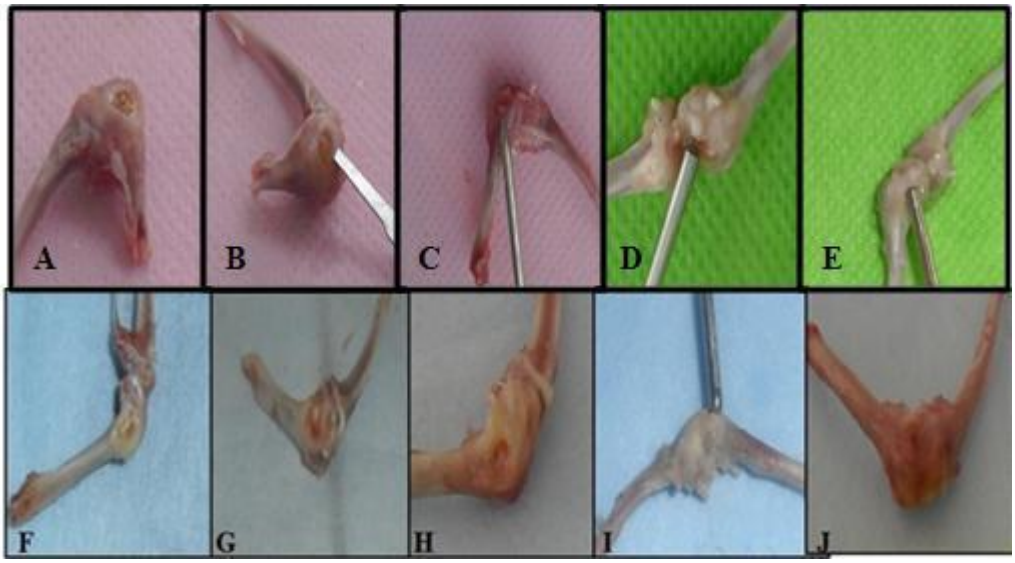

Figures 1. Photographs showing regenerative bone bioglass-chitosan (BG- CH) and bioglass (BG); fibrous tissue at 4, 7 and 15 days in direct contact with BG-CH (A, B, C) and BG (F, G, H,). Significant mineralization defects, at 30 and 60 days in contact with BG-CH (D, E) and BG (I, J).

Table 1. Blood biochemistry for bone metabolism in ovariectomised female Wistar rats (OVX) received bioglass-chitosan (BG-CH) and bioglass (BG).

Parameter	Blood biochemistry			
	T	OVX	OVX –BG-CH	OVX –BG
Ca (mg/dl)	8.70 ± 0.61	9.01 ± 0.41	9.3 ± 0.22	9.02 ± 0.45
P (mg/dl) Si(µg/g)	4.96 ± 0.60	5.04 ± 0.28	4.21 ± 0.9	4.30 ± 0.97
Alkaline activity	0.90±0.26	0.87± 0.21	0.84±0.21	0.85±0.21
Phosphatase (U/L)	383.50±62.7	254.9±90.9*	293 ± 83.75	269.5 ±98.66

Values are expressed as mean ± S.E; *, significant difference compared with controls rats, $p < 0.05$.

bone as well as of the implanted one after different periods (4, 7, 15, 30 and 60 days). Identification of the chemical groups was examined by IR spectroscopy analysis after soaking in 1 mg of material and mixed with dried KBr, using a Bruker Equinox. Femoral condyles were dried for 24 h at 65°C.

Statistical analysis

The statistical analysis of the data was performed using Student's t-test. All values were expressed as means ± SE. Differences were considered significant at the 95% confidence level ($p < 0.05$).

RESULTS

Macroscopic observation

No post-surgery complications were detected in BG and BG-CH after a sixty-day implantation. No osteolysis, hyperplasia or other negative tissue responses were found in the biomaterial samples through the 8-week study. Progressive substitution took place at the interface of implants and host bones were observed (Figure 1).

Biochemical assays

The Ca, P and Si concentration blood values for the experimental and control groups of animals are given in Table 1. These values do not differ from those of the OVX group. Moreover, these concentrations were unaffected by being exposed for 60 days to BG-CH and BG. No adverse effect was observed in clinical examinations through the stability of serum levels of Ca, P and Si. Convincingly, the average blood alkaline phosphate levels of the control groups exceeded 383.5 U/L, whereas in the OVX test groups, they reached only about 254.9 U/L. These levels were found to be significantly reduced. On the other hand no significant changes of alkaline phosphate levels over the post surgical periods seen in OVX-BG-CH and OVX-BG

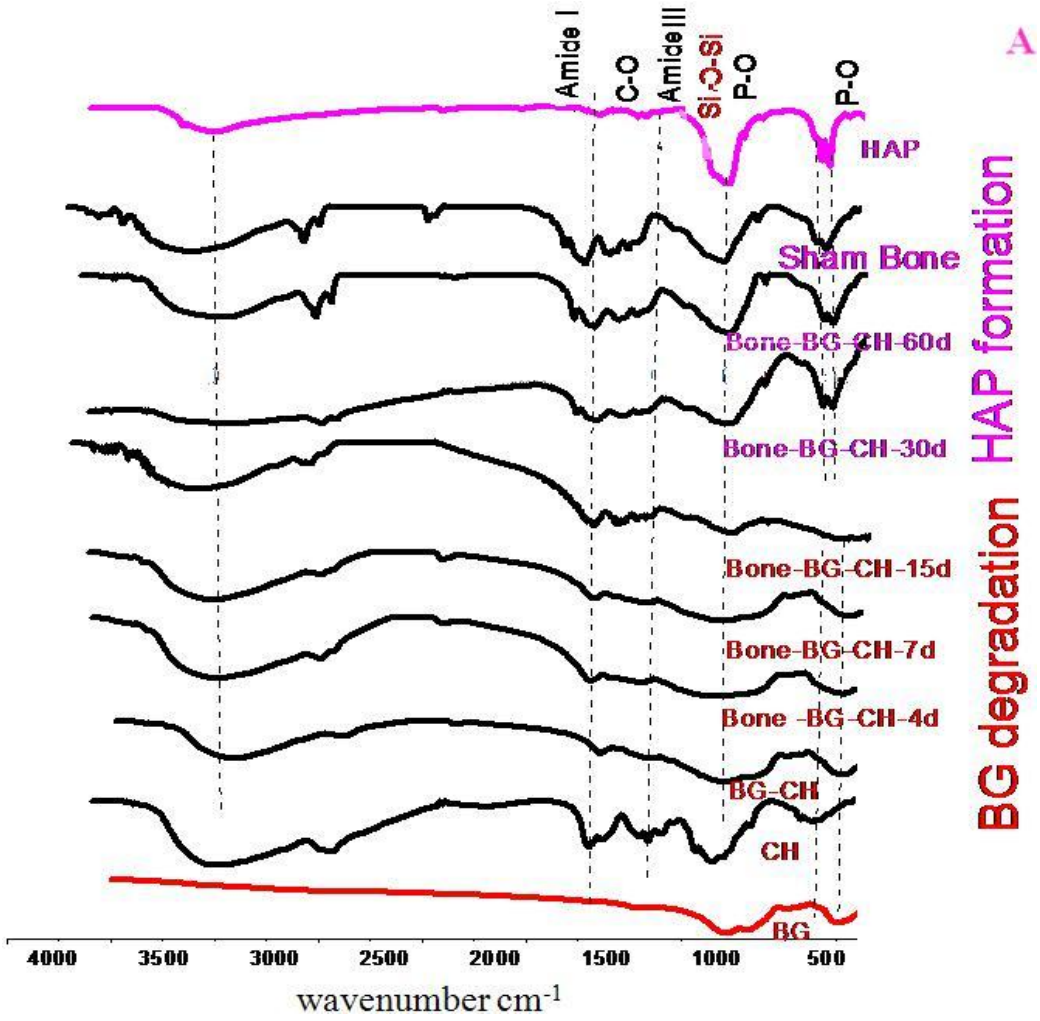

Figures 2A. Infrared spectra from bones implanted by bioglass-chitosan (BG-CH) after 4, 7, 15, 30 and 60 days compared with hydroxyapatite reference spectrum.

groups when compared to T groups.

Physicochemical analysis

FT-IR characterization of specimens after in vivo tests

The spectra in Figure 2A showed as already mentioned absorption bands arising from BG-CH and some new ones. Two pronounced absorption bands with maxima at 932 and 1036 cm^{-1} arising from Si-O-Si groups disappeared 15 days after surgery. These bands were replaced 30 days after implantation by 601 and 564 cm^{-1} (P-O) groups arising from bone apatite. The band at 3572 cm^{-1} could be assigned to hydroxyl groups present in the structure due to BG-CH after 15 days but that probably attributed to bone apatite 60 days after surgery. The absorption band at 1650 cm^{-1} attributed to the stretching (amide I) was also identified. Generally, the amide I bands originate from the (C=O) stretching vibrations coupled to (N-H) bending vibrations (Barth and Zscherp, 2002). Moreover, the band at 1542 cm^{-1} (amide II) arising from the combination of C-N stretching and N-H bending vibrations of the protein bone can be related to protein matrix formation of implanted bone. The carbonate bending vibration groups situated at 1500 to 1418 cm^{-1} were also noticed. These groups were accentuated with a similar intensity to that of a normal bone specially 60 days after surgery. These bands are related to carbonate apatite present in bone tissue, suggesting the presence of mineralized extracellular matrix of bone. We can conclude that the major absorbance bands of IR spectra correspond to apatite bone, increasing significantly as a function of time and the characteristic bands of HA appearing as the BG-CH content decreases. When compared to those of BG (Figure 2B), these bands are more accentuated especially after 60 days of implantation.

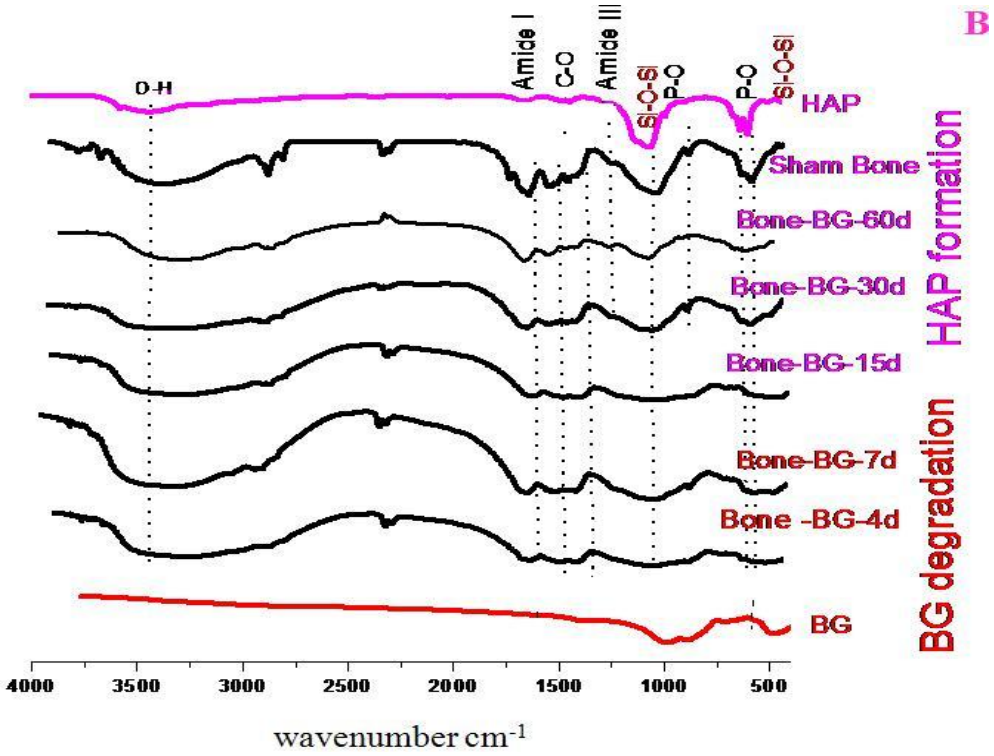

Figure 2B. Infrared spectra from bones implanted by bioglass (BG) after 4, 7, 15, 30 and 60 days compared with hydroxyapatite reference spectrum.

XRD characterization of specimens after the in vivo assays

4 days after surgery, X-ray diagrams of BG-CH-bone suggested the presence of 2 peaks with low intensity at 19.5° (2θ) in (001) orientation and a new one at 29° (2θ) characterizing BG and CH association. We noted there was a characteristic broad hump at 31.5° (2θ) (Figure 3A and B). This broad diffraction pattern is an indication of the predominantly amorphous form of BG-CH. However, 7 days after surgery, peaks at 19.5° and 29° (2θ) disappeared. This transformation exhibited BG-CH fast resorption and degradation behaviour. In this stage, bone tissue can be viewed as a fine layer of organic matrix without deposition of mineral crystals (Figure 3C). After 15 days of implantation, we noted the presence of new sharp diffraction peaks that are the result of new formation at 25.7° (2θ) in (002) orientation (Figure 3D). These peaks show that bone healing is emphasized to provide a stable surface on which osteoblasts and/or their precursor cells may migrate and secrete bone matrix. After 30 days of BG-CH exposure, minerals were deposited within collagen fibers in which large amounts of solid mineral crystals were deposited as shown in Figure 3E, and the registered peaks were more developed. After 60 days, the evaluation of the crystallinity was performed especially by the analysis of (002) and (221) line profile in implanted bone (Figure 3F). The implanted bone was presented in the same way as normal bone and the degrees of calcification seemed to be enhanced. XRD analysis in combination with IR spectroscopy studies indicated that the formation of HAP was more accentuated in BG-CH when compared with BG especially 15 days after surgery.

SEM observation

Under scanning electron microscopy, Figure 4 allows to visualize the pore network. It was observed that BG-CH had average pore sizes of approximately 10 µm in diameter. Pores could be expected to afford space for bone in growth. The defect was mainly filled with fibrous connective tissue and callus detected 4 days after operation. Little haematoma appeared around the specimens 7 days after surgery. In contrast, BG was surrounded by a great deal of haematoma in the same period (Figure 5A and B). The implant was partitioned and a minimal cellular invasion emerged in 7 days. During the next 2 weeks, the BG-CH was replaced by creeping substitution and a mature newly generated bone appeared at the defect site. In the newly formed bone biological HAP was deposited in an orderly way on a collagenous matrix as we noted the biodegradation of BG –CH (Figure 6A and B). BG-CH have been shown to encourage cell spreading and improve the ability and

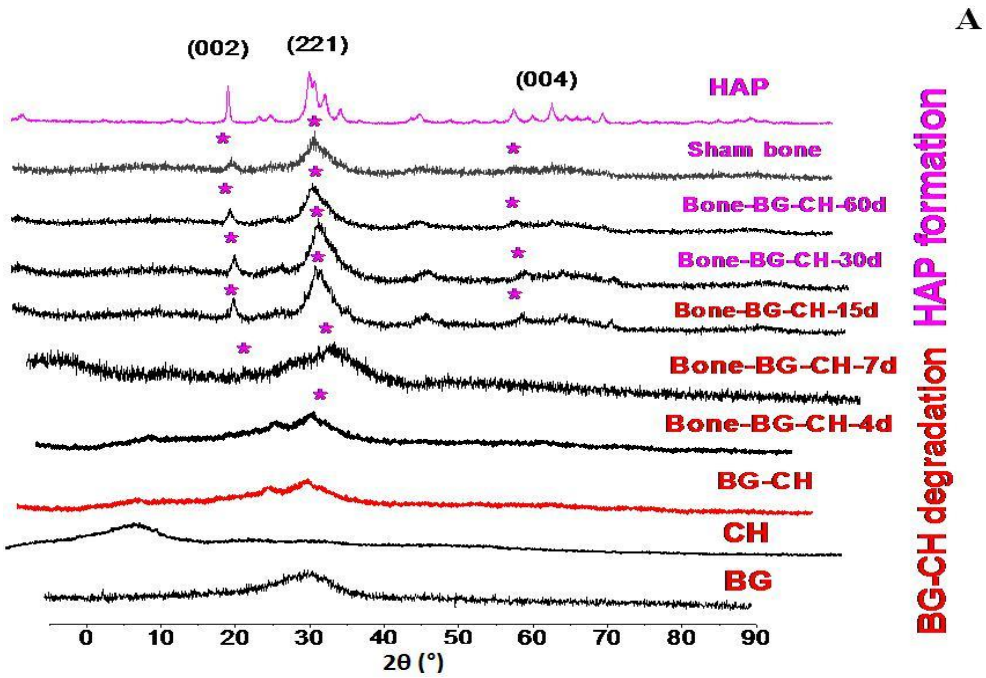

Figure 3A. X-ray diffraction from bones implanted by bioglass-chitosan (BG-CH) after 4, 7, 15, 30 and 60 days compared with hydroxyapatite reference spectrum.

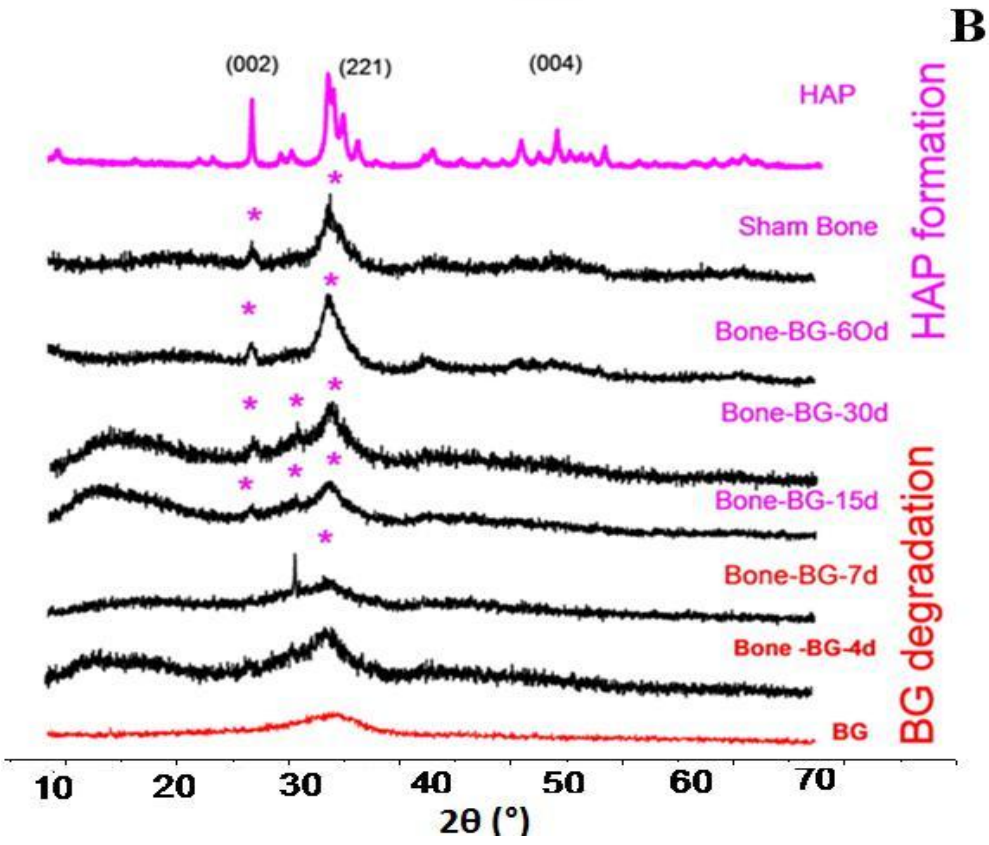

Figure 3B. X-ray diffraction from bones implanted by bioglass (BG) after 4, 7, 15, 30 and 60 days compared with hydroxyapatite reference spectrum.

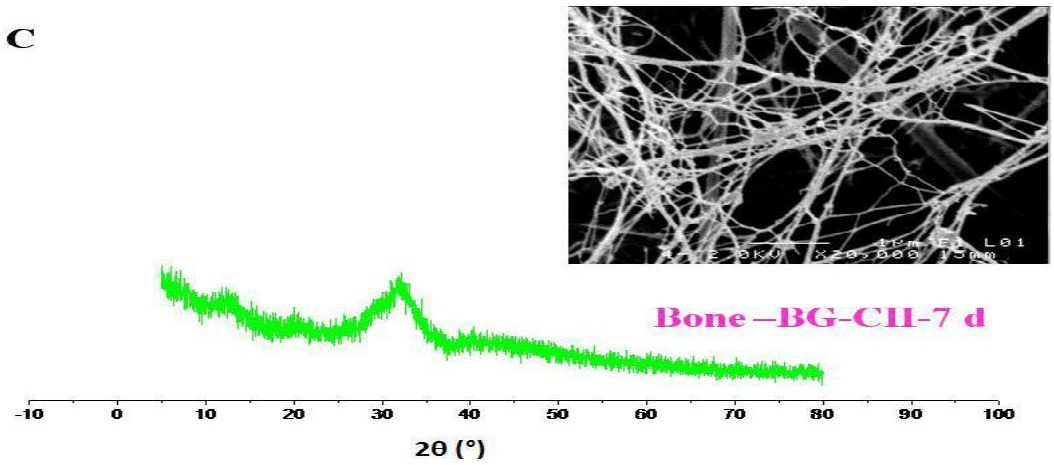

Figure 3C. Immature bone tissue after 7 days of implantation and poor crystallinity demonstrated by X-ray diffraction analysis.

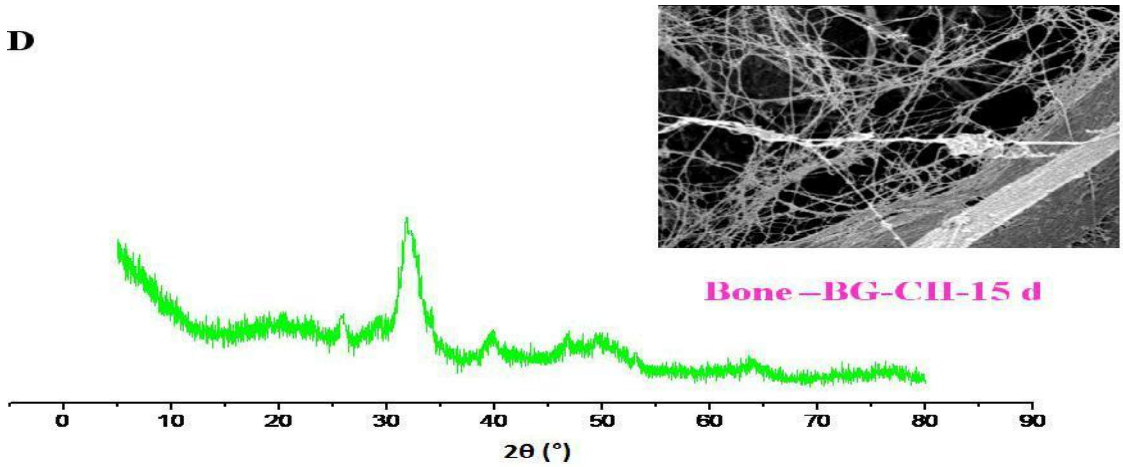

Figure 3D. Early stages of bone tissue mineralization and advanced stage of crystallinity after 15 days of implantation demonstrated by X-ray diffraction analysis.

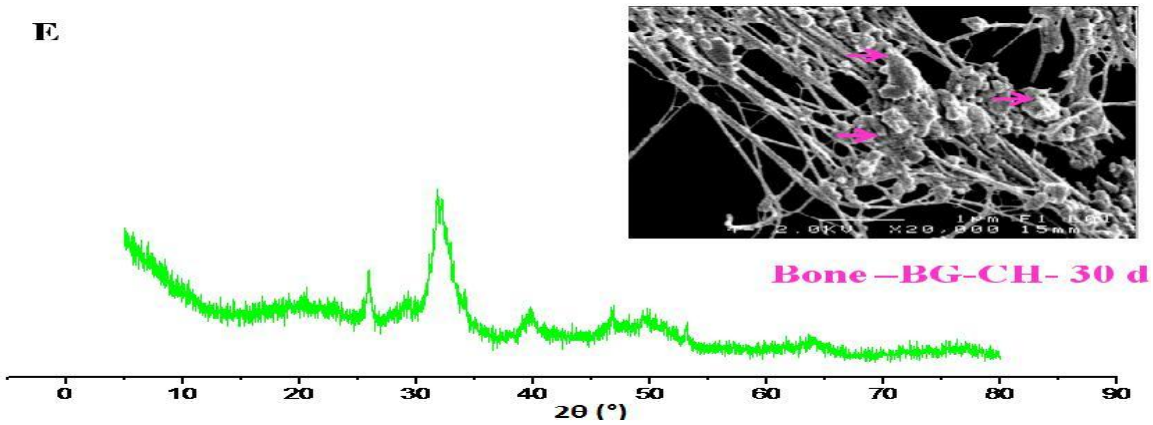

Figure 3E. Disturbance of mineral crystals among collagen (SEM observation) after 30 days (d) of implantation confirmed crystallinity of bone tissue as shown by X-ray diffraction analysis.

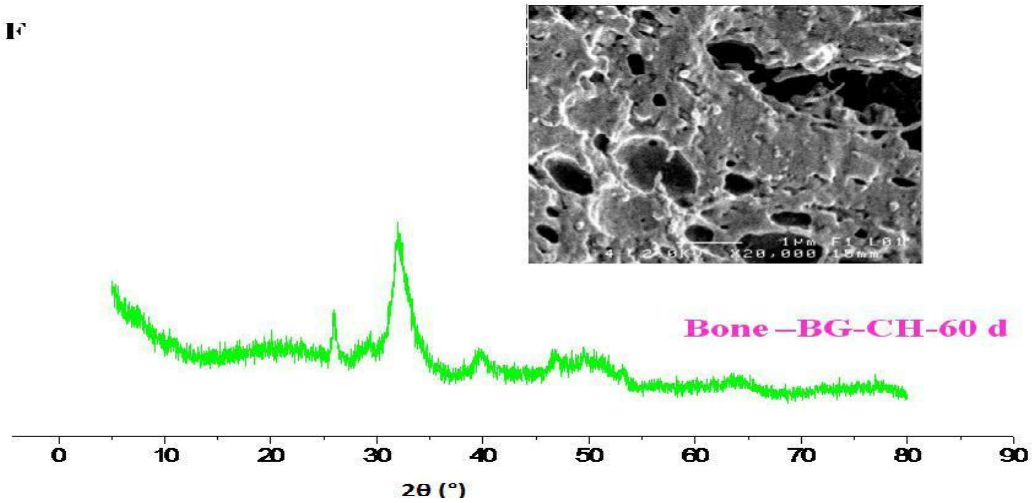

Figure 3F. Advanced stages of bone tissue mineralization confirmed by X-ray diffraction analysis.

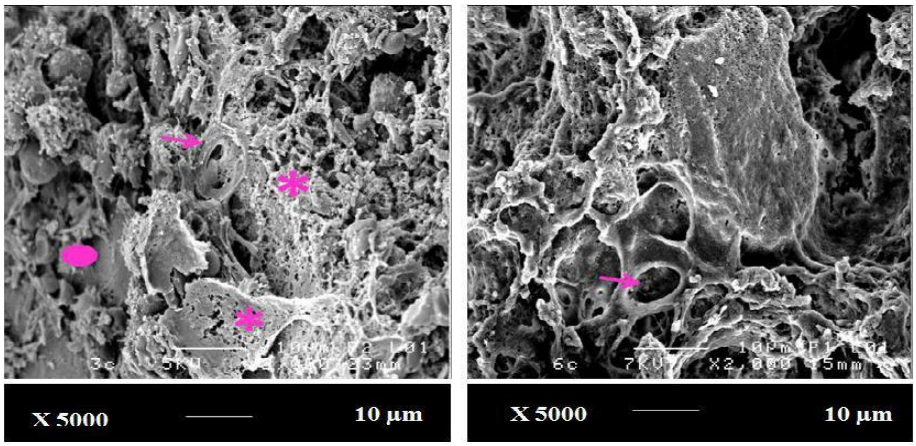

Figure 4. SEM image of bone–implant in female Wistar rat 7 days post surgery. * Indicates BG-CH osseointegration. Arrows point indicates BG-CH pore. Circle indicates bone.

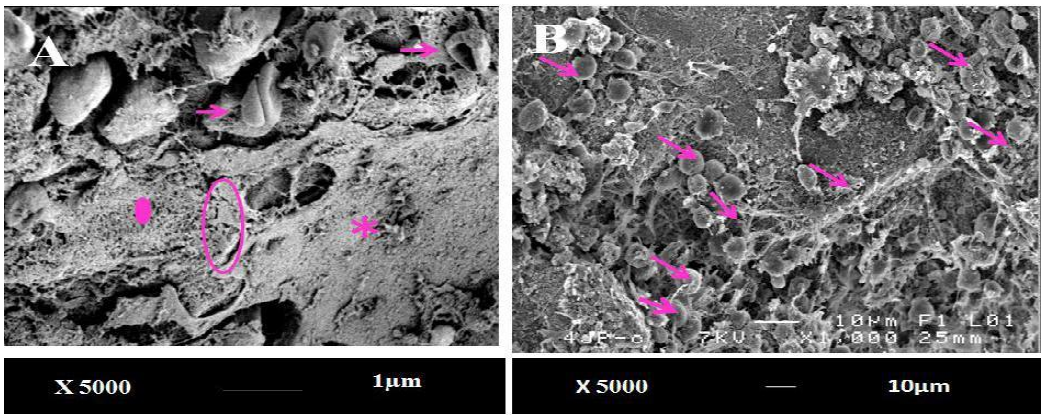

Figure 5. SEM image of *in vivo* erythrocyte adhesion on bioglass-chitosan BG-CH (A); Less hematoma shown on BG-CH than bioglass BG (B) after 7 days of implantation. Circle indicates BG-CH osseointegration. Arrows point indicates erythrocyte cells and point indicates bone.

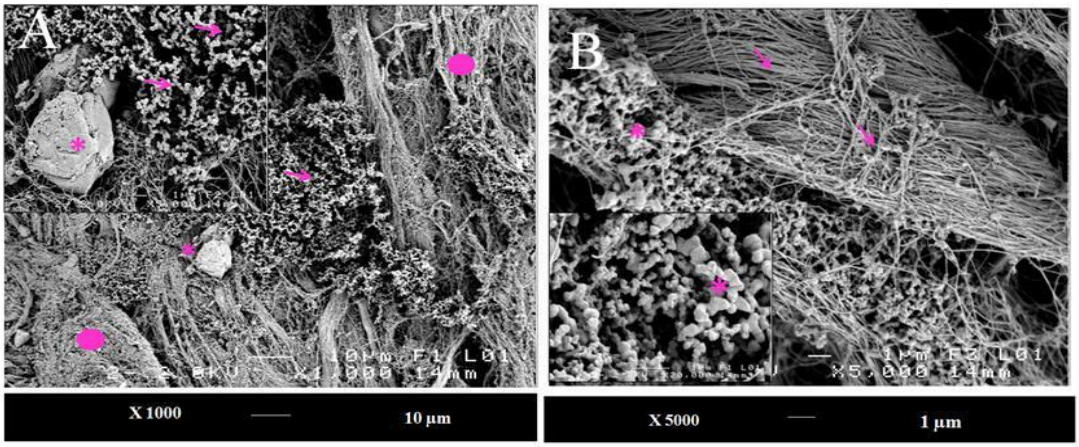

Figure 6. Bioglass-chitosan (BG-CH) biodegradation (A) and disturbance of mineral crystals among the collagen fibrils of bone (B). * indicates biodegraded BG-CH after 30 days of implantation. Arrows point indicates mineral crystals of hyroxyapatite. Circle indicates bone. + indicates collagens.

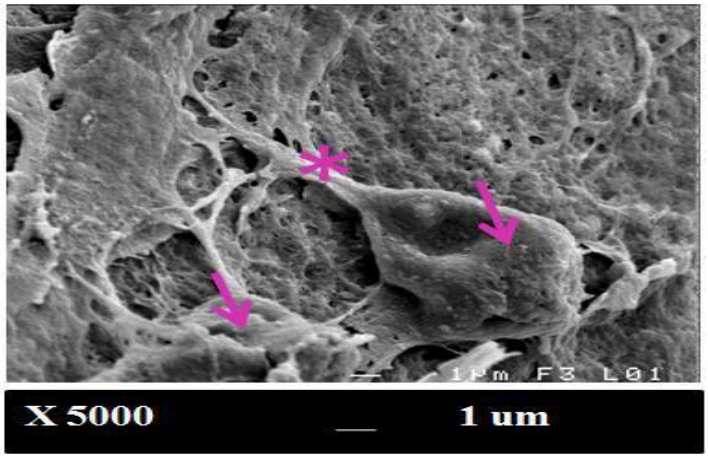

Figure 7. Active cells spread to neighboring cells. Arrows point indicates cells and * indicates cell-cell interconnection.

interconnection with neighboring cells (Figure 7). In 4 weeks, a big amount of original osseous callus was formed, whereas some defect regions were still occupied by implant. These features demonstrate that BG-CH is safe, well tolerated by the host and the in growth becomes more pronounced with increasing time periods of implantation. New bone progressively forms on the implants surface and incorporates into the host bone showing that BG-CH has excellent biocompatibility and has proven effective in osseointegration.

DISCUSSION

In the biomedical field, CH is considered to be osteoconductive as well as osteoinductive. It stimulates osteoprogenitor cells in surrounding tissue and supporting new bone growth along the bone–implant (Salgado et al., 2004). On the other hand, BG is classified as osteoconductive (Nandi et al., 2009). Moreover, HAP formed from BG proved to have great resemblance with living HAP (Zhou et al., 2004). Oudadesse et al. (2011) have worked on the formulation of CH and BG composite for use as a bone-graft substitute. This proposed composite showed i*n vitro* that particles were not cytotoxic to SaOS2 cells line and promoted differentiation. The amalgamation of polymer with mineral is used to give a composite that has the toughness and flexibility of the polymer with the strength and hardness of the mineral filler (Chen et al., 2011). In addition to *in vitro* studies, it is essential to implant them *in vivo* to know body reactions. The present study aimed

to test the degradability and bone forming capacity of BG-CH. *In vivo* parameters such as inflammatory response, tissue ingrowth, vascularization give the correct evidence to consider the BG-CH biofunctionality. After implantation of any biomaterial, the host tissue will inevitably be traumatized by the implantation procedure (Mikos et al., 1998). An inflammatory response triggered by BG-CH particle was observed after 1 week of bone implantation. 60 days after surgery, no systemic or regional surgical complications were seen. Under optical microscopy, it is clear that BG-CH architecture allowed for tissue ingrowth and subsequent migration into and through the matrix. BG-CH increased the bone contact perimeter and the neoformed bone became mature more quickly. There was no fibrose along with the repair processes since fibrose is the main reason of inflammation (Idris et al., 2011). Furthermore, calcium is an indicator of the level of mineral deposition, and it is considered as a marker of the full maturation of osteoblastic cells (Wanga and Ma, 2002). At the end of the third week, the calcium measure-ments in the newly formed bone indicated the deposition of significant amounts of mineralized matrix, with a significant increase for Ca-P. This layer may display the characteristics of bioactivity which allows them to form a chemical bond with the bone tissue resulting in a very strong bone/ BG-CH interface. The BG-CH influence on the structure of the HA-like conversion product remains unclear (Rahaman et al., 2011). The addition of 17 wt% CH provides cationic sites to BG, which helps to give an electrostatic interaction with the negative charges on the cell surface such as glycosaminoglycans (GAG),

proteoglycans and other negatively charged molecules.This property is very interesting because most cytokines/growth factors are linked to GAG (mostly with heparin and heparan sulphate) (Pillai et al., 2009). The association between BG-CH complex and GAG may retain and concentrate growth factors secreted by colonizing cells (Li et al., 1999). Moreover, in recent study, authors found that CH inhibited the resorption activity (Kurita, 2001). Our findings confirm that CH helps to prevent bone loss after ovariectomy. Pore size is another important factor for tissue ingrowth. Among the most common techniques to create porosity in biomaterial are salt leaching, gas foaming, phase separation and freeze-drying which is the method used to create porosity in BG-CH. The porosity of 10 µm could be viewed in BG-CH by SEM. It is believed to contribute to high bone inducing protein adsorption as well as to ion exchange and bone-like apatite formation (Yuan et al., 1999). Previous studies reported that a broad distribution of pore sizes (10 to 300 µm) helped to regenerate bone in femoral defects in rabbits (Itala et al., 2001). Based on early studies, migration requirements and nutrient transport required 100 µm of pore size. Although increased porosity and pore size facilitate bone ingrowth, the result is a reduction in mechanical properties. Porosity in combination with the presence of a bioactive material could have a synergic effect and may be responsible for improvements in material colonization by cells. Another appropriate characteristic of chitosan is the capacity of wound healing (Antonov et al., 2008). BG-CH seemed to be considered as an accelerator of wound healing by playing a role in the infiltration of polymorphonuclear cells at the wound site. Much less haematoma appeared in the BG-CH specimens than that of BG at the end of 1 week. Many researchers admit that the hemostatic effects of CH are related to both platelets and erythrocyte aggregations (Wu et al., 2008). The ionic attraction between negatively charged red blood cell membranes and positively charged groups in CH is a possible explanation for the anticoagulant activity of chitosan. On the other hand, in blood plasma of OVX - BG-CH content Si and Ca comes to normal. Based on early studies, the Si diffuses into the local tissue and then enters the blood or lymph to be distributed to other parts of the body in a soluble form (Baumann, 1960). The silicon will finally be filtered out of the blood by the kidney (Laia et al., 2002). During this dissolution, the silicon concentration in the organs and body fluids remains within physiologically safe ranges. Moreover, our study aimed to contribute to this research by evaluating the physicochemical properties that suggest the BG-CH influence on the mineral crystal maturation. Ovariectomy induced a decrease in carbonate band as demonstrated in literature (Fei et al., 2007). FTIR spectra of the reacted material after implantation show the development of bands attributable to carbonate groups. It may be considered as a significant factor in controlling the size of apatite crystals in skeletal tissues by inducing proliferative growth of new crystals (Farlay et al., 2010).The association between the BG and CH showed the appearance of a new peak at 29°. It highlights the chemical interactions between bioactive glass and chitosan polymers which induce the changes in the glass amorphous structure. After 4 days of implantation, we noted a small quantity of carbonate but 60 days after surgery, the spectrum exhibited an increase of carbonate at 1063 cm^{-1} indicating bone maturity. X-ray diffraction pattern showed that reaction time is sufficiently long for BG-CH to induce peaks corresponding to HA but this layer is not homogenous as shown by SEM. A possible explanation is that the conversion reaction does not proceed in a continuous manner (Huang et al., 2006). Instead, it starts and stops, presumably depending on the concentration of the reacting ions from BG-CH. By 60 days, we obtained peaks close to the normal bone. The crystal formation is the final stage and it is considered as an important event in the multistep process of hard tissue formation. These results indicate that shortly after implantation, bone apatite is poorly crystallized. In fact, trabecular bone from ovariectomized rats contained larger apatite crystals (Boyar and Severcan, 2003). The process of bone mineral deposition begins with the nucleation of HA crystals at multiple sites on the collagen

fibrils (Fratzl et al., 1991). In bone, extracellular matrix proteins act as nucleators because of their affinity for HA. Finally, the 60 days of implantation suggest that within the osteoid tissue, there is an increase in crystal content, and perfection of mineralization proceeds. Thus, as a function of time the introduction of BG-CH enhances the secondary mineralization which is associated with an increase in the crystal size as well as the mineral content as shown by XRD results

Conclusion

Under these experimental conditions, both BG-CH and BG seemed to promote an excellent structural response in terms of bone integration. The combination of 17 wt% of CH with BG was shown to maximize the biocompatibility and the osteoinonductive behavior *in vivo*. The chemical transformations of BG-CH reflect the positive effect on the crystal maturity during ossification. These studies added that BG-CH materials were promising candidates for bone repair requirements. However, this study was limited to only an 8-week investigation and needs to be an in-depth study of longer time implantation in the future.

REFERENCES

Antonov SF, Kryzhanovskaya EV, Yu I, Filippov S, Shinkarev M, Frolova MA (2008). Study of wound-healing properties of chitosan. Vet. Sci., 34: 426-427.

Barth A, CH Zscherp (2002). What vibrations tell us about proteins. Q Rev. Biophys., 4: 369–430.

Baumann H (1960). Behavior of silica acid in human blood and urine. Physiol. Chem., 320: 11-20

Boyar H, Severcan F (2003). FTIR spectroscopic investigation of mineral structure of streptozotocin induced diabeticrat femur and tibia. Spectroscopy Int. J., 17: 627-633.

Chang J, Liu W, Han B, Liu B (2008). Biological proprieties of chitosan films with different degree of deacetylation. J. Mater. Sci. Technol., 24: 700-708.

Chen J, Zhang G, Yang S, Li J, Jia H, Fang Z, Zhang Q (2011). Effects of in situ and physical mixing on mechanical and bioactive behaviors of nano hydroxyapatite-chitosan scaffolds. J. Biomater. Sci. Polym. Ed., 22: 2097-2106

Dietrich E, Oudadesse H, Lucas-Girot A, Mami M (2009). In vitro bioactivity of melt-derived glass 46S6 doped with magnesium, J. Biomed. Mater. Res. A., 88: 1087-1096.

Farlay D, Panczer G, Rey C, Delmas DP, Boivin G (2010). Mineral maturity and crystallinity index are distinct characteristics of bone mineral, J. Bone. Miner. Metab., 28 : 433–445.

Fei Y, Zhang M, Li M, Huang Y, He W , Ding W, Yang J (2007). Element analysis in femur of diabetic osteoporosis model by SRXRF microprobe. Micron, 38: 637–642.

Fratzl P, Fratzl-Zelman N, Klaushofer K, Vogl G, Koller K (1991). Nucleation and growth of mineral crystals in bone studied by small-angle X-ray scattering Calc. Tissue Int., 48: 407-413.

Grady D, Rubin SM, Petitti DB, Fox CS, Black D, Ettinger B, Ernster VL, Cummings SR (199l). Hormone therapy to prevent disease and prolong life in postmenopausal women. Ann. Int. Med., 117: 1016-1037.

Ha K-B, Son W-S, Kim S-W (2001). Effect of estrogen and progesterone on the proliferation and activity of osteaoblastic cells. Korean J. Orthod., 31: 237-248

Huang w, Day DE, Kittiratanapiboon K, Rahaman MN (2006). Kinetics and mechanisms of the conversion of silicate (45S5), borate, and borosilicate glasses to hydroxyapatite in dilute phosphate solutions. J. Mater. Sci. Mater. Med., 17: 583-596.

Idris SB, Bolstad AI, Ibrahim SO, Danmark S, Finne-Wistrand A, Albertsson AC, et al (2011). Global Gene Expression Profile of Osteoblast-Like Cells Grown on Polyester Copolymer Scaffolds. Tissue Eng. Part A., 17: 2817-2831.

Itala AI, Ylanen HO, Ekholm C, Karlsson KH, Aro HT (2001). Pore diameter of more than 100 micron is not requisite for bone ingrowth in rabbits, J. Biomed. Mater. Res., 58: 679–683.

Iwata H, Yana S, Nasu M, Yosue T (2005). Effects of chitosan oligosaccharides on the femur trabecular structure in ovariectomized rats. Oral Radiol., 21: 19–22.

Kashiwazaki H, Kishiya Y, Matsuda A, Yamaguchi K, Iizuka T, Tanaka J, Inoue N (2009). Fabrication of porous chitosan/hydroxyapatite nanocomposites: their mechanical and biological properties. Biomed. Mater. Eng., 19:133-140.

Kurita K (2001). Controlled functionalization of the polysaccharide chitin, Progr. Polym. Sci., 26: 1921–1971.

Laia W, Garinob J, Ducheynea P (2002). Silicon excretion from bioactive glass implanted in rabbit bone. Biomaterials, 23:213–17.

Lee HS, Hong SG, Kim JG (1999). Experimental study on the effects of ovariectomy and estrogen on the bone pattern of mandible in rats, Korean J. Orthod., 29: 83-94.

Li H, Miyahara T, Tezuka Y, Watanabe M, Nemoto N, Seto H, Kadota S *(*1999). The effect of low molecular weight chitosan on bone resorption *in vitro* and *in vivo.* Phytomedicine, 6: 305–310.

Liuy J, Shi F, Yu L, Niu L, Gao SH (2009). Synthesis of chitosan-hydroxyapatite composites and its effect on the properties of bioglass bone cement. J. Mater. Sci. Technol., 25: 551-555.

Malafaya PB, Santos TC, Griensven van M, Reis RL (2008) Morphology, mechanical characterization and i*n vivo* neo vascularization of chitosan particle aggregated scaffolds architectures. Biomaterial, 29 : 3914-3926.

Mikos AG, McIntire LV, Anderson JM, Babensee JE (1998). Host response to tissue engineered devices. Adv. Drug .Deliv. Rev., 33: 111–139.

Muzzarelli RAA, Mattioli-Belmonte M, Miliani M, Muzzarelli C, Gabbanelli F, Biagini G (2002). In vivo and in vitro biodegradation of oxychitin–chitosan and oxypullulan–chitosan complexes. Carbohydr. Polym., 48: 15-21.

Nandi SK, Kundu B, Mukherjee P, Mandal TK, Datta S, De DK, *et al (*2009). In vitro and in vivo release of cefuroxime axetil from bioactive glass as an implantable delivery system in experimental osteomyelitis, Ceram. Int., 35: 3207–3216

Oudadesse H, Bui XV, Le Gal Y, Mostafa A, Cathelineau G (2011).Effects on Bioactive Glass for Application as Biocopmosite Biomaterial. Int. J. Biol. Biomed. Eng., 5: 49-56.

Petera M, Binulal NS, Naira SV, Selvamurugana N, Tamurac H , Jayakumara R (2010). Novel biodegradable chitosan–gelatin/nano-bioactive glass ceramic composite scaffolds for alveolar bone tissue engineering. Chem. Eng. J., 158: 353-361.

Pillai CKS, Paul W, Sharma CP (2009).Chitin and chitosan polymers: Chemistry, solubility and fiber formation, Progr. Polym. Sci., 34: 641–78.

Rahaman MN, Day DE, Bal BS, Q Fu , SB Jung , LF Bonewald , Tomsia AP *(*2011). Bioactive glass in tissue engineering. Acta. Biomat., 7: 2355-2373.

Rani M, Agarwal A, Maharana T, Negi YS (2010). A comparative study for interpenetrating polymeric network (IPN) of chitosan-amino acid beads for controlled drug release. Afr. J. Pharm. Pharmacol., 4: 035-054.

Rochet N, Balaguer T, Boukhechba F, Laugier JP, Quincey D , Goncalves S (2009). Differentiation and activity of human preosteoclasts on chitosan enriched calcium phosphate cement. Biomaterials, 30: 4260- 4267.

Salgado AJ, Coutinho OP, RL Reis (2004). Bone tissue engineering: state of the art and future trends, Macromol. Biosci., 4: 743-765

Viral HS, Pragna S, Gaurang BSH (2012). Design and evaluation of thiolated chitosan based mucoadhesive and permeation enhancing bilayered buccal drug delivery system. Afr. J. Pharm. Pharmacol., 7:

491-501.
Wanga X, Ma J (2002). Bone repair in radii and tibias of rabbits with phosphorylated chitosan reinforced calcium phosphate cements. Biomaterial, 23: 4167-4176.
Wu Y, Hu Y, Cai J,S. Ma, Wang X (2008).Coagulation property of hyaluronic acid–collagen/chitosan complex film. J. Mater. Sci. Mater. Med., 19: 3621–3629.
Yuan H, Kurashina K, De Bruijn JD, Li Y, Groot De K, Zhang X (1999). A preliminary study on osteoinduction of two kinds of calcium phosphate ceramics. Biomaterial, 201: 799–806.
Zhang J, Xia W, Liu P, Cheng Q, Tahirou T, Gu W, Li B (2010). Chitosan Modification and Pharmaceutical/Biomedical Applications Mar. Drugs, 8: 1962-1987.
Zhou Q Fu N, Huang W, Wang D, Zhang L (2004). Formation and Characterization of Bone-like Nanoscale. Hydroxyapatite in Glass Bone Cement. J. Mater. Sci. Technol., 20: 702-774